A New Experimental Procedure for Determining the Response of Bolometric Detectors to Fields in Any State of Coherence

Christopher N. Thomas[1*], Stafford Withington[1], and George Saklatvala[1]

[1]*Detector and Optical Physics Group, Cavendish Laboratory, JJ Thomson Avenue, Cambridge, CB3 OHE, UK*

* Contact: c.thomas@mrao.cam.ac.uk

***Abstract*— Any bolometer that is greater than a few wavelengths in size is receptive to the power in a number of fully coherent optical modes simultaneously. Knowing the amplitude, phase, and polarisation patterns of these modes, and their relative sensitivities, is central to being able to use a multimode detector effectively. We describe a procedure for measuring the spatial state of coherence to which a detector is sensitive. Diagonalisation of the coherence function then gives the natural modes. The scheme is based on the result that the expectation value of the output of any detector, or indeed whole instrument or telescope, is given by the contraction of two tensor fields: one of which describes the state of coherence of the incoming radiation, and the other describes the state of coherence to which the detector is sensitive. It follows that if a detector is illuminated by two coherent point sources, in the near or far field, and the phase of one source rotated relative to the other, the output of the detector displays a fringe. By repeating the process with different source locations, the detector's coherence tensor can be reconstructed from the recorded complex visibilities. This new, powerful technique is essentially aperture synthesis interferometry in reverse, and therefore many of the data processing techniques developed in the context of astronomy can be used for characterising the optical behaviour of few-mode bolometers.**

I. INTRODUCTION

The use of bolometric detectors in far-infrared and submillimetre astronomy is now widespread. In many instruments, the bolometers are antenna-coupled [1] – for example, Planck-HFI [2] and CLOVER [3] – meaning that an absorber loads a single-mode antenna, which in turn illuminates a telescope. The advantage of this arrangement is that it is well known how single-mode antennas couple to optical systems, allowing precise control of the beam pattern on the sky. In fact, because the system is single-mode, it is straightforward to propagate the beam pattern of the detector through the optical system, and onto the sky. In the case of large-format imaging arrays, however, there is a tendency to use free-space absorbing pixels. This configuration can give full, instantaneous sampling of the sky, and high absorption efficiency in a number of optical modes simultaneously. A major problem, however, is that the optical coupling between the telescope and detector is poorly understood, and there is no obvious way of fully characterising the reception pattern, largely because it is partially coherent. It is tempting to treat these systems in a similar way to CCDs in optical astronomy, and assume that each pixel is simply re-imaged on the sky. This approximation assumes the incident field is fully spatially incoherent, and that the pixel collects, on a point-by-point basis, all of the radiation that is incident on it: sometime called a 'light bucket'. The radiation in a telescope at a particular frequency, although thermal in origin, is spatially correlated over length scales of at least a wavelength by virtue of the free-space Maxwell's equations, which only allow spatial variations over scales sizes of greater than a wavelength, and only allow divergence-free fields: combined these give black body radiation. Additional correlations may be introduced by the telescope optics. In an optical telescope, the pixels are typically much larger then a wavelength, and so the incoherent approximation holds. In far-infrared and submillimetre astronomy, however, the dimensions of the pixels are similar to a wavelength, which is typically the same as the coherence length, including polarization, of the radiation. To understand how a bolometer couples to a telescope, we therefore need a way of characterising the response of multimode detectors to fields in any state of spatial coherence.

In this paper, we describe an experimental technique for determining quantitatively the sensitivity of bolometric detectors to fields in any state of spatial coherence. We begin by introducing a parameterisation of a bolometer's behaviour in terms of the set of modes to which it is sensitive; this gives rise to a response function, which can be used to characterise the behaviour of any detector or complete system. Next we describe how two phase-locked, coherent, radiation sources can be used to measure the response function experimentally. Finally we discuss experimental apparatus that is being constructed to demonstrate and develop this method. In order to have numerical simulations against which the experimental data can be compared, we will present work that has been carried out on modelling the response function of free-space planar absorbers. Our model emphasises diffractive effects caused by the finite size of the absorber, and which, to first order,

can be considered independent of the specific absorption mechanism at work. A sharp change from multi- to few-mode behaviour is observed when the dimensions of the absorber become smaller than the wavelength of the radiation being absorbed.

It is worth emphasising that the methods described are very general, and can be applied any type of bolometer or system, at any wavelength. For example, it should be possible to distinguish between the behaviour of pixels having continuous thin films as absorbers, and pixels having frequency-selective surfaces, such as tightly packed arrays of thin-film dipoles. Further, although the emphasis is on characterising the behaviour of single, free-space bolometers, the same technique can be applied to systems such as imaging arrays and phased arrays. In the case of measurements on antenna-coupled bolometers, which are theoretically single-mode, it is possible that the technique will reveal other unexpected ways for radiation to couple power into the absorbing element. For example, the incident radiation might cause ohmic heating of a planar antenna, which is then conducted to the bolometer. Many other effects, such as surface waves, might contribute.

II. PARAMETERISING BOLOMETER RESPONSE

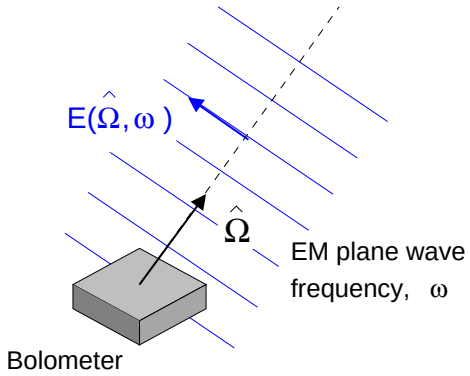

Fig. 1 A bolometer being illuminated with monochromatic plane wave radiation. The notation used in the theoretical discussion is illustrated.

To begin with, a way of parameterising the relationship between the state of spatial coherence of the incident radiation and the output of the detector is needed. This problem has been addressed by Saklatvala and Withington in [4] and [5]. They have shown that is possible to characterise a bolometer in terms of a set of fully coherent modes of the incident field in which the detector is simultaneously sensitive to power, along with a set of coefficients that describe the relative influence of each of the modes on the detector's output. We outline the approach here. In this paper we will consider only incident radiation that is statistically stationary. In this situation, the power absorbed at different wavelengths can be treated independently, and at each wavelength there is a different set of spatial modes and coefficients. It is also possible to deal with non-stationary fields, but this requires spatio-temporal modes and these will not be discussed here.

Consider a bolometer being illuminated by monochromatic plane radiation with frequency ω as shown in Fig. 1. The incident field is described by a vector function $\mathbf{E}(\hat{\mathbf{\Omega}},\omega)$ which gives the complex electric field amplitude of the plane wave incident from the direction $\hat{\mathbf{\Omega}}$. Consider for the moment replacing the bolometer with a classical antenna. The net power, $P(\omega)$, absorbed by the antenna from the field would be given by:

$$P(\omega) = \left| \int_S d^2\hat{\mathbf{\Omega}}\ \mathbf{R}^*(\hat{\mathbf{\Omega}},\omega)\cdot\mathbf{E}(\hat{\mathbf{\Omega}},\omega) \right|^2 , \qquad (1)$$

where $\mathbf{R}(\hat{\mathbf{\Omega}},\omega)$ is called the antenna reception pattern [6] and the integral is taken over all possible incidence directions. Equation (1) is simply the full vector form of more familiar antenna reception relations. A classical antenna is an example of a single-mode detector. Equation (1) simply describes mathematically the process of determining the power carried in the single mode – described by $\mathbf{R}(\hat{\mathbf{\Omega}},\omega)$ – by the incident field. The logical extension of (1) to multimode-detectors is:

$$p(\omega) = \sum_n \gamma^{(n)} \left| \int_s d^2\hat{\mathbf{\Omega}}\ \mathbf{U}^{(n)*}(\hat{\mathbf{\Omega}},\omega)\cdot\mathbf{E}(\hat{\mathbf{\Omega}},\omega) \right|^2 , \qquad (2)$$

where $p(\omega)$ is the detector output. The $\{\ \mathbf{U}^{(n)}(\hat{\mathbf{\Omega}},\omega)\ \}$ are the set of fully coherent modes of the field in which the detector is simultaneously sensitive to power. We shall refer to these modes as the natural optical modes of the detector. As modes, they are 'orthogonal' to one another in the sense

$$\int_S d^2\hat{\mathbf{\Omega}}\ \mathbf{U}^{(m)*}(\hat{\mathbf{\Omega}},\omega)\cdot\mathbf{U}^{(n)}(\hat{\mathbf{\Omega}},\omega) = \delta_{mn} . \qquad (3)$$

In (3) we have further assumed that the modes are individually normalised. The set of coefficients $\{\gamma^{(n)}\}$ quantify how the output of the bolometer changes with the power in each mode. The set of normalised coefficients, $\{\gamma^{(n)} / \Sigma_m \gamma^{(m)}\}$, gives, therefore, an indication of the relative responsivity to the power in each mode. In the case where the incident field is partially coherent, we can take the ensemble average, $\langle\ \rangle$, of (2) to obtain

$$p(\omega) = \int_S d^2\hat{\mathbf{\Omega}}_1 \int_S d^2\hat{\mathbf{\Omega}}_2 \left(\sum_n \gamma^{(n)} \mathbf{U}^{(n)*}(\hat{\mathbf{\Omega}}_1,\omega)\mathbf{U}^{(n)}(\hat{\mathbf{\Omega}}_2,\omega) \right)^{\dagger} \cdot\cdot \left\langle \mathbf{E}^*(\hat{\mathbf{\Omega}}_1,\omega)\mathbf{E}(\hat{\mathbf{\Omega}}_2,\omega) \right\rangle , \qquad (4)$$

where we have expanded out the norm. The double-dot denotes two scalar products, one between the inner pair of vectors followed by one between the outer pair. The natural modes of the detector can be taken outside the ensemble average because we have assumed previously they are fully coherent. Defining the dyadic fields

$$\overline{\overline{D}}(\hat{\boldsymbol{\Omega}}_1,\hat{\boldsymbol{\Omega}}_2,\omega)=\sum_n \gamma^{(n)}\mathbf{U}^{(n)*}(\hat{\boldsymbol{\Omega}}_1,\omega)\mathbf{U}^{(n)}(\hat{\boldsymbol{\Omega}}_2,\omega) \qquad (5)$$

and

$$\overline{\overline{E}}(\hat{\boldsymbol{\Omega}}_1,\hat{\boldsymbol{\Omega}}_2,\omega)=\left\langle \mathbf{E}^*(\hat{\boldsymbol{\Omega}}_1,\omega)\mathbf{E}(\hat{\boldsymbol{\Omega}}_2,\omega)\right\rangle, \qquad (6)$$

which is the cross-spectral density of the incident field, equation (4) becomes

$$p(\omega)=\int_S d^2\hat{\boldsymbol{\Omega}}_1\int_S d^2\hat{\boldsymbol{\Omega}}_2\ \overline{\overline{D}}^{\dagger}(\hat{\boldsymbol{\Omega}}_1,\hat{\boldsymbol{\Omega}}_2,\omega)\cdot\cdot\,\overline{\overline{E}}(\hat{\boldsymbol{\Omega}}_1,\hat{\boldsymbol{\Omega}}_2,\omega), \qquad (7)$$

which reproduces the results of Saklatvala and Withington, which were derived in a more rigorous way. We see that provided $\overline{\overline{D}}(\hat{\boldsymbol{\Omega}}_1,\hat{\boldsymbol{\Omega}}_2,\omega)$ is known, it is possible to calculate the output of a detector when it is subjected to any illuminating field. We shall thus take $\overline{\overline{D}}(\hat{\boldsymbol{\Omega}}_1,\hat{\boldsymbol{\Omega}}_2,\omega)$, which we shall refer to as the *detector response function*, as our parameterisation of the detector behaviour. A useful physical interpretation of the meaning of $\overline{\overline{D}}(\hat{\boldsymbol{\Omega}}_1,\hat{\boldsymbol{\Omega}}_2,\omega)$ can be obtained by taking the ensemble average of (1), expanding the norm and using (6) to obtain

$$p(\omega)=\int_S d^2\hat{\boldsymbol{\Omega}}_1\int_S d^2\hat{\boldsymbol{\Omega}}_2\left\langle \mathbf{R}^*(\hat{\boldsymbol{\Omega}}_1,\omega)\mathbf{R}(\hat{\boldsymbol{\Omega}}_2,\omega)\right\rangle^{\dagger}\cdot\cdot\,\overline{\overline{E}}(\hat{\boldsymbol{\Omega}}_1,\hat{\boldsymbol{\Omega}}_2,\omega) \qquad (8)$$

We see that the detector response function corresponds to the cross-spectral density of the reception pattern. We can therefore think of it as describing the state of spatial coherence of the field to which the bolometer is sensitive. In the special case of an antenna, this field is fully-coherent. In the case of a multimode detector, it is partially coherent and the natural optical modes of the detector correspond to what are known as the coherent modes of the field [7].

In the next section we will discuss how the detector response function can be determined experimentally. However, sometimes is also useful to know the natural optical modes of the detector. Although no single reception pattern exists for a multimode bolometer, we can propagate the optical modes of the detector though the telescope to find a set of beam patterns on the sky to which the bolometer is independently sensitive. The natural optical modes of the detector can be found by solving the following equation:

$$\int_S d^2\hat{\boldsymbol{\Omega}}_2\ \overline{\overline{D}}(\hat{\boldsymbol{\Omega}}_1,\hat{\boldsymbol{\Omega}}_2,\omega)\cdot\mathbf{U}^{(n)}(\hat{\boldsymbol{\Omega}}_2,\omega)=\gamma^{(n)}\mathbf{U}^{(n)}(\hat{\boldsymbol{\Omega}}_1,\omega) \qquad (9)$$

This is an eigenfunction equation. We see that the $\gamma^{(n)}$ that describe the responsivity of the detector to the power in each mode are the eigenvalues of the detector response function.

III. EXPERIMENTAL DETERMINATION OF THE DETECTOR RESPONSE FUNCTION

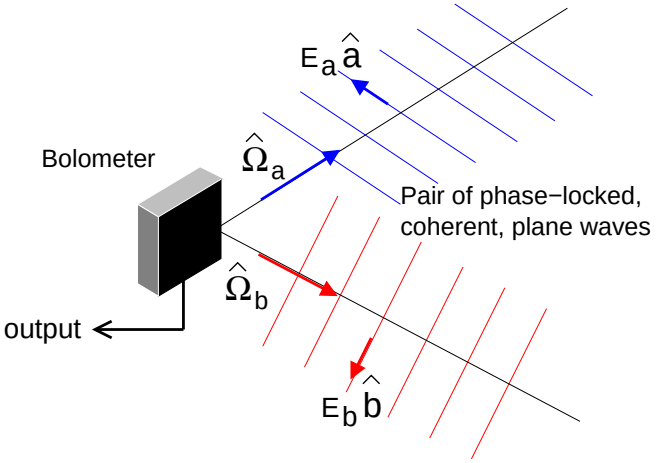

Fig. 2 Diagram of the characterisation procedure. An element of the detector response function can be obtained from the visibility of the fringes in the output signal that result from rotating the phase difference between the incident waves.

Consider placing two monochromatic, point-like, radio sources operating at the same frequency, ω_0, in the far field of a detector. Assume that the sources are individually fully coherent and, further, that they are phase-locked to one another with a controllable differential phase angle, $\Delta\psi$. They produce, at the detector, a pair of phase-locked plane waves, as shown in Fig. 2. The polarisation states, amplitude and direction of incidence of the waves depend on the source positions and orientations. For the plane waves shown in Fig. 2, the incident field is of the form

$$\mathbf{E}(\hat{\boldsymbol{\Omega}},\omega_0)=E_a\,\hat{\mathbf{a}}\,\delta(\hat{\boldsymbol{\Omega}}-\hat{\boldsymbol{\Omega}}_a)+E_b\,e^{i\Delta\psi}\,\hat{\mathbf{b}}\,\delta(\hat{\boldsymbol{\Omega}}-\hat{\boldsymbol{\Omega}}_b) \qquad (10)$$

Substituting (10) into (7) we obtain

$$\begin{aligned}\left\langle p(\omega)\right\rangle = {} & E_a^2\,D_{aa}(\hat{\boldsymbol{\Omega}}_a,\hat{\boldsymbol{\Omega}}_a,\omega_0)\\ & +E_b^2\,D_{bb}(\hat{\boldsymbol{\Omega}}_b,\hat{\boldsymbol{\Omega}}_b,\omega_0)\\ & +E_a\,E_b\,e^{i\Delta\psi}D_{ab}(\hat{\boldsymbol{\Omega}}_a,\hat{\boldsymbol{\Omega}}_b,\omega_0)\\ & +E_a\,E_b\,e^{-i\Delta\psi}D_{ba}(\hat{\boldsymbol{\Omega}}_b,\hat{\boldsymbol{\Omega}}_a,\omega_0)\end{aligned}, \qquad (11)$$

where we have used the shorthand for the matrix elements

$$D_{ab}(\hat{\mathbf{\Omega}}_a,\hat{\mathbf{\Omega}}_b,\omega_0)=\hat{\mathbf{a}}\cdot\overline{\overline{D}}(\hat{\mathbf{\Omega}}_a,\hat{\mathbf{\Omega}}_b,\omega)\cdot\hat{\mathbf{b}}\,. \qquad (12)$$

From (5) we have that

$$D_{ab}(\hat{\mathbf{\Omega}}_a,\hat{\mathbf{\Omega}}_b,\omega_0)=D^*_{ba}(\hat{\mathbf{\Omega}}_b,\hat{\mathbf{\Omega}}_a,\omega_0)\,. \qquad (13)$$

We can also argue that (13) must be true as otherwise we see from (11) that the detector output would depend on the way the plane waves are labelled, which is arbitrary. Using (13) we can simplify (11) to

$$\begin{aligned}\langle p(\omega)\rangle = {} & E_a^2\,D_{aa}(\hat{\mathbf{\Omega}}_a,\hat{\mathbf{\Omega}}_a,\omega_0)\\ & + E_b^2\,D_{bb}(\hat{\mathbf{\Omega}}_b,\hat{\mathbf{\Omega}}_b,\omega_0)\\ & + 2\,E_a\,E_b\left|D_{ab}(\hat{\mathbf{\Omega}}_a,\hat{\mathbf{\Omega}}_b,\omega_0)\right|\\ & \times\cos\left(\Delta\psi+Arg(D_{ab}(\hat{\mathbf{\Omega}}_a,\hat{\mathbf{\Omega}}_b,\omega_0))\right)\end{aligned}\,. \qquad (14)$$

Consequently as the phase angle between the sources, $\Delta\psi$, is rotated we expect the output of the detector to show fringes, as in Fig. 3. Provided we know E_a and E_b, from the amplitude and phase of this fringe pattern, we can determine both the modulus and phase of $D_{ab}(\hat{\mathbf{\Omega}}_a,\hat{\mathbf{\Omega}}_b,\omega_0)$. From (13) it also follows that we measure $D_{ba}(\hat{\mathbf{\Omega}}_b,\hat{\mathbf{\Omega}}_a,\omega_0)$. By repeating this process with different source locations – to change the incidence angle of the plane waves – and different source orientations – to change the wave polarisations – it is possible to map out the detector response function in full and characterise the bolometer. Subsequently, we can obtain the natural optical modes of the detector by solving (9).

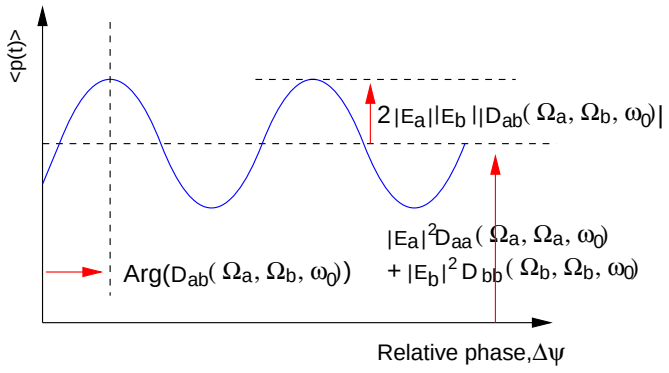

Fig. 3 Expected form of the output in Fig. 1 when the phase difference between the illuminating waves is rotated.

It might appear that a large number of measurements will be needed to characterise a device, but this is not the case. Consider an example where we are trying to sample the detector response function over a set of N different illumination directions. Naively we might expect to have to make $\sim 2N^2$ measurements. There are N illumination directions with two possible polarisation states in each case, giving $(2N)^2$ possible arrangements of two sources. However, because of (13) we only need to measure half of these combinations. In fact, the actual number of degrees of freedom is fixed by the number of modes, n, of the incident field in which the detector is sensitive to power. From (5) we expect the number of degrees of freedom in the values measured to be $\sim(2N+1)n$, corresponding to $2N$ degrees of freedom per mode plus an additional n degrees of freedom in the $\gamma^{(n)}$. When n is less than N, there are fewer degrees of freedom than measurements and the system is highly constrained. It should therefore be possible to impute the full set of data from a smaller subset of measurements.

We are currently investigating an imputation strategy based on work of Brand [8], who worked on imputing missing values in matrices of data. In the case of sampled data, the detector response function reduces to a matrix, with the missing values corresponding to readings not taken yet. Brand's algorithm was originally intended for use in online recommender systems for retail, where it would be used to fill in missing product reviews based on the incomplete reviews supplied by the user. There are two reasons why his strategy is particularly attractive to us. Firstly, it imputes the missing values so that the completed matrix has the lowest rank – i.e. degrees of freedom – possible. Secondly, because it is intended to be used online, it has been designed so that the imputed values can be updated in linear time as new data arrives. It should therefore be possible to calculate the prediction in real time as the experiment is performed; updating the current best estimate as additional scans are performed. Although there are many possibilities, basically speaking, once the singular values have converged, we will know that we have taken sufficient data and can stop.

There are also other methods available for reducing the number of measurements that need to be taken. Up to this point we have discussed characterising the response of the bolometer to plane-wave illumination from all possible directions. In practical applications, however, the illumination angles are likely to be restricted, and it obviously makes sense to only characterise the detector over its working range. Equation (9) can be solved over this restricted range of illumination angles to find the set of detector natural modes over the restricted region. These are likely to be different to the natural modes over the full range of incidence directions, but can be used equivalently. This approximation saves greatly on the number of measurements needed.

IV. EXPERIMENTAL VALIDATION OF THE TECHNIQUE

We plan to demonstrate the validity of the proposed technique by using it to investigate the power reception characteristics of planar absorbing structures with dimensions similar to or smaller than the wavelength of the illuminating radiation. In this section, we will describe the experimental

system, and theoretical work we have been doing to predict the behaviour that should be seen.

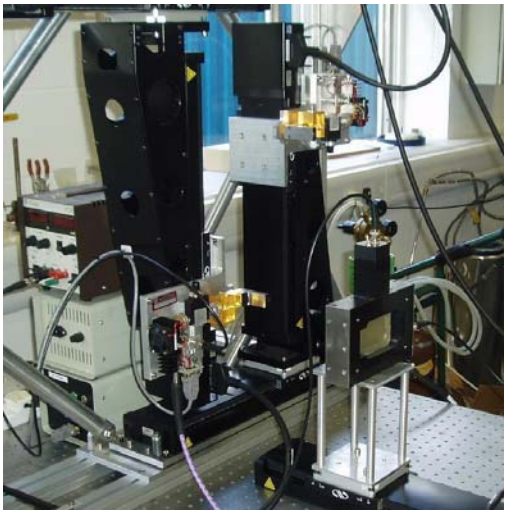

Fig. 4 Photo of the system being developed to perform the characterisation measurements. The object in the foreground is a test sensor for checking the operation of the sources. In the background, the powered slides and sources can be seen.

Fig. 4 is a photograph of the apparatus in its current form. We are using two, 195-270GHz sources, which are mounted on powered slides to allow different illumination angles. The sources can also be rotated manually to allow different polarisation angles. In practise, rather then operating the sources at the same frequency, as suggested previously, we instead intend to drive them at slightly different frequencies, with the offset derived from a common reference. The idea is that if the offset frequency is sufficiently small, the field that results will approximate two plane waves at the same RF frequency whose relative phase varies periodically in time. The advantage of this approach is that the need for a separate phase shifter is eliminated. In its more extreme form, where the difference frequency is scanned over a large range, the full spatio-temporal state of coherence of the detector's response can be found.

In the foreground of Fig. 4, a calibration detector from Thomas Keating Ltd can be seen, which we are using to check the operation of the basic instrument. The detector is mounted on a powered slide to allow the distance between the sources and the detector to be modulated, which will allow the effects of standing-waves to be removed. Our early experiments will simulate planar absorbers of different dimensions by placing appropriate apertures over the face of the detector. Later, we hope to use a range of room-temperature detectors, based on suspended Si_xN_y islands, similar to the structures used for Transition Edge Sensors. A schematic of the design is shown in Fig. 5. An advantage of this approach is that we will be able to study the behaviour of many different configurations, and some of the designs can be close to the geometries used in ultra-low-noise free-space-coupled bolometers.

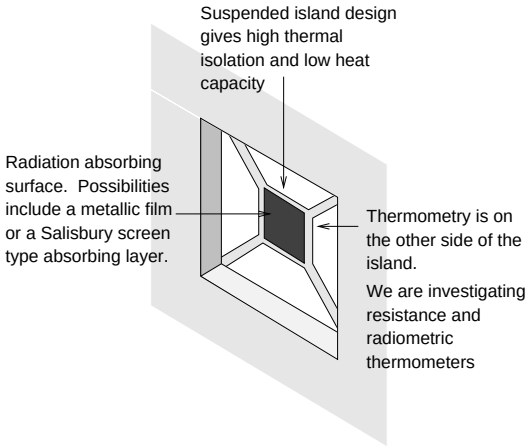

Fig. 5 Concept drawing for model planar bolometer for use in the validation experiments described. The design is based on a suspended silicon nitride island structure and it is intended to operate it at room temperature.

V. THEORETICAL MODEL OF A PLANAR BOLOMETER

In this section, we describe work that has been done on modelling the detector response function of planar bolometers. The purpose of the study was to develop numerical simulations against which experimental data can be compared. Out intention was to investigate the way in which performance of a planar bolometer is influenced by its size, independent of the specific power absorption mechanism at work. To this end we assumed the absorption mechanism was 'ideal', so that our model represents in some way, the best possible performance obtainable from a 'real' detector of the same dimensions.

A. Details of Model

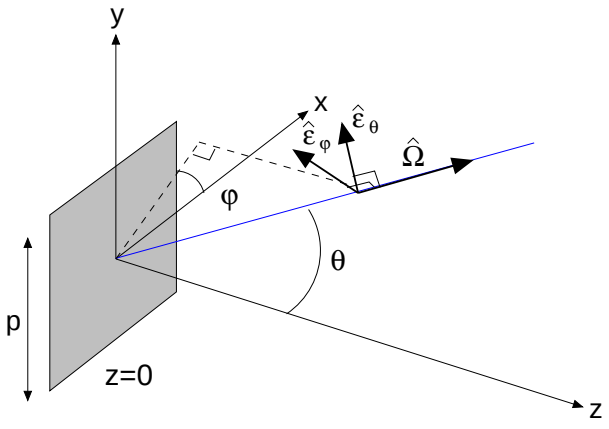

Fig. 6 Diagram illustrating the model pixel considered and the notation used in the theoretical discussion.

Fig. 6 shows the model planar bolometer and defines the notation that we will use. We have only considered bolometers with a square absorbing surface. It would, however, be easy to apply similar techniques to a planar bolometer of a different shape. We denote the side-length of the square by p and the wavelength of the radiation by λ. For simplicity we assume the absorber occupies the region of the $z = 0$ plane defined by $|x| \leq p/2$ and $|y| \leq p/2$.

Until now we have considered the response of the bolometer to incident plane waves. However, when modelling an ideal planar bolometer it is actually much easier to work in terms of its response to the electric field over the plane containing it. We denote this field $E_{z=0}(\mathbf{r},\omega)$, where $\mathbf{r} = (x, y)$ is a point lying in the plane z = 0. In the preceding analysis of the far field detector behaviour, the detector was characterised in terms of a set of field modes in which it is simultaneously sensitive to power. The same approach can be used to characterise its response to fields over the plane. We assume the detector is simultaneously responsive to the power in a set of modes of the field over the plane, given by $\{\mathbf{V}^{(n)}{}_{z=0}(\mathbf{r},\omega)\}$. Further, we assume there is a set of coefficients $\{\beta^{(n)}\}$ that, like the $\gamma^{(n)}$, quantify how much the output scales with the power in the associated mode. We can then define a function

$$\overline{\overline{D}}_{z=0}(\mathbf{r}_1,\mathbf{r}_2,\omega) = \sum_n \beta^{(n)} \mathbf{V}^{(n)*}(\mathbf{r}_1,\omega)\mathbf{V}^{(n)}(\mathbf{r}_2,\omega), \qquad (15)$$

which is the equivalent of the detector response function for fields on the plane. As such it describes the state of spatial coherence of the field over the plane to which the bolometer is sensitive. The equivalent of expression (7) for the fields over the bolometer plane is

$$p(\omega) = \int_{z=0} d^2\mathbf{r}_1 \int_{z=0} d^2\mathbf{r}_2 \, \overline{\overline{D}}^{\dagger}_{z=0}(\mathbf{r}_1,\mathbf{r}_2,\omega) \cdot\cdot \overline{\overline{E}}_{z=0}(\mathbf{r}_1,\mathbf{r}_2,\omega), \qquad (16)$$

where $\overline{\overline{E}}_{z=0}(\mathbf{r}_1,\mathbf{r}_2,\omega)$ is the cross-spectral density of the plane electric field. An ideal bolometer is sensitive to the total power incident over its surface. This requires the detector output be proportional to the intensity of the field integrated over the absorber surface, or

$$p(\omega) \propto \int_{\substack{\text{absorber}\\ \text{surface}}} d^2\mathbf{r} \left|E(\mathbf{r},\omega)\right|^2 . \qquad (17)$$

From (16) we see that this requires that $\overline{\overline{D}}_{z=0}(\mathbf{r}_1,\mathbf{r}_2,\omega)$, be of the form

$$\overline{\overline{D}}_{z=0}(\mathbf{r}_1,\mathbf{r}_2,\omega) = \begin{cases} C\,\delta(\mathbf{r}_1 - \mathbf{r}_2) & \mathbf{r}_1 \text{ and } \mathbf{r}_2 \text{ on absorber} \\ 0 & \text{otherwise} \end{cases}, \qquad (18)$$

where C is a proportionality constant.

The important question now is how the detector response function, $\overline{\overline{D}}_{z=0}(\mathbf{r}_1,\mathbf{r}_2,\omega)$, is related to $\overline{\overline{D}}(\hat{\boldsymbol{\Omega}}_1,\hat{\boldsymbol{\Omega}}_2,\omega)$. We will present a simple argument for the expected form. Our approach is based on the relationship between the reception pattern of a classical aperture antenna and the field over the aperture plane to which it is sensitive. Denoting the reception pattern by $\mathbf{R}(\hat{\boldsymbol{\Omega}},\omega)$ as before and the aperture field as $\mathbf{R}_{z=0}(\mathbf{r},\omega)$, we have

$$\mathbf{R}(\hat{\boldsymbol{\Omega}},\omega) = -\frac{2\pi i}{k}\cos\theta\,(\overline{\overline{I}} - \hat{\boldsymbol{\Omega}}\hat{\boldsymbol{\Omega}}^*)\cdot \int_{z=0} d^2\mathbf{r}\,\mathbf{R}_{z=0}(\mathbf{r},\omega)\,e^{-ik\hat{\boldsymbol{\Omega}}\cdot\mathbf{r}}, \qquad (19)$$

where we have used the notation in Fig. 5. This result follows from the equivalence between the reception pattern of a classical and its transmission pattern. Equation (19) simply represents the process of propagating a field from a plane to the far field, using standard methods [6]. This raises a point, which will be important later. As (19) is a propagation equation, we see that the reception pattern/far-field sensitivity of the antenna is determined only by the component of the aperture field that is able to propagate. This is most easily separated out in the angular spectrum domain. The angular spectrum of the aperture field is given by

$$A(\mathbf{k}_t,\omega) = \frac{1}{2\pi}\int_{z=0} d^2\mathbf{r}\,\mathbf{R}(\mathbf{r},\omega)\,e^{-i\mathbf{k}_t\cdot\mathbf{r}} . \qquad (20)$$

Essentially it is the 2D spatial Fourier transform of the field. We see that the angular spectrum appears in (19) in a rewritten form and that each spatial frequency component can be associated with a particular plane wave, the vector associated with that component giving the vector amplitude of the wave. The propagating component of the field satisfies the following in the angular spectrum domain:

I. $|\mathbf{k}_t| \leq k$. If $|\mathbf{k}_t| \geq k$ the wave associated with a spatial component is evanescent. In (19) this filtering is intrinsic to the expression. Since $\mathbf{k} = k\hat{\boldsymbol{\Omega}}$ and $\hat{\boldsymbol{\Omega}}$ is a unit vector, $|\mathbf{k}_t|$ is always limited to being less than k.

II. Electromagnetic waves are transverse polarised, so only components of the polarisation vector normal to the wave direction can propagate. This component can be found by acting on the vector with $(\overline{\overline{I}} - \hat{\boldsymbol{\Omega}}\hat{\boldsymbol{\Omega}}^*)$, as in (19).

The first step corresponds to spatially low-pass filtering the field, which means the propagating component cannot vary on length scales smaller than λ. We will see the implication of this shortly.

In our model, we assume the detector response function is given by

$$\overline{\overline{D}}(\hat{\mathbf{\Omega}}_1,\hat{\mathbf{\Omega}}_2,\omega)=\sum_n \beta^{(n)}\mathbf{V}^{(n)*}(\hat{\mathbf{\Omega}}_1,\omega)\mathbf{V}^{(n)}(\hat{\mathbf{\Omega}}_2,\omega), \qquad (21)$$

where the $\{\boldsymbol{V}^{(n)}(\hat{\mathbf{\Omega}},\omega)\}$ are the set of natural optical modes of the detector, $\{\boldsymbol{V}^{(n)}_{z=0}(\boldsymbol{r},\omega)\}$, transformed according to (19). Essentially, we treat the planar bolometer as a set of aperture antennas and assume that the plane wave response of the detector can be found simply from the plane wave response of these modes. This seems sensible. Despite the similarity of (21) to (5), the transformed natural modes of the field on the plane will not necessarily correspond to the far field natural modes of the detector. This is because the transformation does not, in general, preserve orthogonality and so there is no guarantee the transformed modes will satisfy (3), in which case they do not form a valid set of far field modes. To find the far-field modes, (9) must instead be solved for the response function constructed from (21). Expanding (21) with (20) and using (15) to simplify, we obtain

$$\begin{aligned}\overline{\overline{D}}(\hat{\mathbf{\Omega}}_1,\hat{\mathbf{\Omega}}_2,\omega)&=\frac{4\pi^2}{k^2}\cos\theta_1\cos\theta_2\\ &\times\int_{z=0} d^2\mathbf{r}_1\int_{z=0} d^2\mathbf{r}_2\; e^{-ik\hat{\mathbf{\Omega}}_1\cdot\mathbf{r}_1}\; e^{ik\hat{\mathbf{\Omega}}_2\cdot\mathbf{r}_2}\\ &\times(\bar{\bar{I}}-\hat{\mathbf{\Omega}}_1\hat{\mathbf{\Omega}}_1^*)\cdot\overline{\overline{D}}_{z=0}(\mathbf{r}_1,\mathbf{r}_2,\omega)\cdot(\bar{\bar{I}}-\hat{\mathbf{\Omega}}_2\hat{\mathbf{\Omega}}_2^*)\end{aligned}, \qquad (22)$$

which relates the response on the plane to the detector response function that we would measure in an experiment. We find the detector response function for our ideal bolometer by substituting (18) into (22). This integral has already been done by Withington [9] for the purpose of modelling the optical behaviour of bolometric focal plane imaging arrays. Withington treats the bolometer as a perfect black body absorber, which is essentially what we have done. Chuss [10] has developed this work and has considered the field patterns on the sky to which a complete telescope is sensitive. Using their results for this integral, we obtain finally for the detector response function of the ideal bolometer:

$$\begin{aligned}\overline{\overline{D}}(\hat{\mathbf{\Omega}}_1,\hat{\mathbf{\Omega}}_2,\omega)&=\eta(\omega)\cos\theta_1\cos\theta_2\\ &\times\operatorname{sinc}\left(\frac{p\pi}{\lambda}\hat{\mathbf{x}}\cdot(\hat{\mathbf{\Omega}}_1-\hat{\mathbf{\Omega}}_2)\right)\\ &\times\operatorname{sinc}\left(\frac{p\pi}{\lambda}\hat{\mathbf{y}}\cdot(\hat{\mathbf{\Omega}}_1-\hat{\mathbf{\Omega}}_2)\right)\\ &\times(\bar{\bar{I}}-\hat{\mathbf{\Omega}}_1\hat{\mathbf{\Omega}}_1^*)\cdot(\bar{\bar{I}}-\hat{\mathbf{\Omega}}_2\hat{\mathbf{\Omega}}_2^*)\end{aligned}, \qquad (23)$$

where we have grouped miscellaneous proportionality constants into the factor η(ω).

It was noted earlier that $\overline{\overline{D}}_{z=0}(\mathbf{r}_1,\mathbf{r}_2,\omega)$ describes the state of spatial coherence of the field over the plane to which the detector is sensitive. From (18), we hence see that in our model we have assumed the coherence length of this field is zero over the absorber surface. However, this picture of the coherence length of the reception field is complicated slightly when we consider propagating radiation fields. From (22) and the discussion of (20), we see that the far-field behaviour of the detector, i.e. its response to propagating radiation, depends only on the propagating component of the field represented by $\overline{\overline{D}}_{z=0}(\mathbf{r}_1,\mathbf{r}_2,\omega)$. This may also be seen by considering (16) in the angular spectrum domain for an incident field that satisfies the two propagation criteria from earlier. As discussed before, higher order spatial frequencies are absent from the propagating component. For monochromatic fields, this limits the smallest scale over which the propagating can vary to distances on the order of a wavelength, λ. This is important for partially coherent fields, as it means that the coherence length of the propagating component cannot be $< \lambda$. This result holds regardless of the coherence length of the full field. Since incoming radiation can only interact with the propagating component of $\overline{\overline{D}}_{z=0}(\mathbf{r}_1,\mathbf{r}_2,\omega)$, from the point of reference of the radiation the coherence length of the reception field therefore appears to be ~λ. We shall refer to this coherence length as the *apparent* coherence length of the reception field. This is to distinguish it from the actual coherence length of the reception field, which is zero in the model. The actual coherence length depends of the physics of the radiation absorption process. The apparent coherent length has important implications, which will be seen in the next section.

B. Modal Behaviour of the Model Detector

Equation (9) was solved numerically with the response function of (23) to find the natural optical modes of the model detector and the associated eigenvalues for several different values of the ratio p/λ. For all values of this ratio, the model bolometer was found to be responsive to the same set of modes. This set resembles the spherical vector harmonics, but multiplied in each case by an additional factor of the cosine of the zenith angle, θ. As p/λ is varied, what changes is the relative responsivity of the model planar bolometer to each mode in the set rather then the modes' spatial forms. In general it was also observed that the responsivities vary with p/λ in such a way that the ordering of the modes based on associated eigenvalue, $\gamma^{(n)}$, is preserved.

Fig. 7 illustrates how the response of the detector to each mode varies over the range $p/\lambda = 0.25 - 4.0$. For each value of p/λ, the thirty-five largest normalised eigenvalues, $\{\gamma^{(n)}/\Sigma_m \gamma^{(m)}\}$, of the response function are plotted in descending order. Although in reality the eigenvalues for each value of p/λ are a discrete set, in the plot I have joined the points

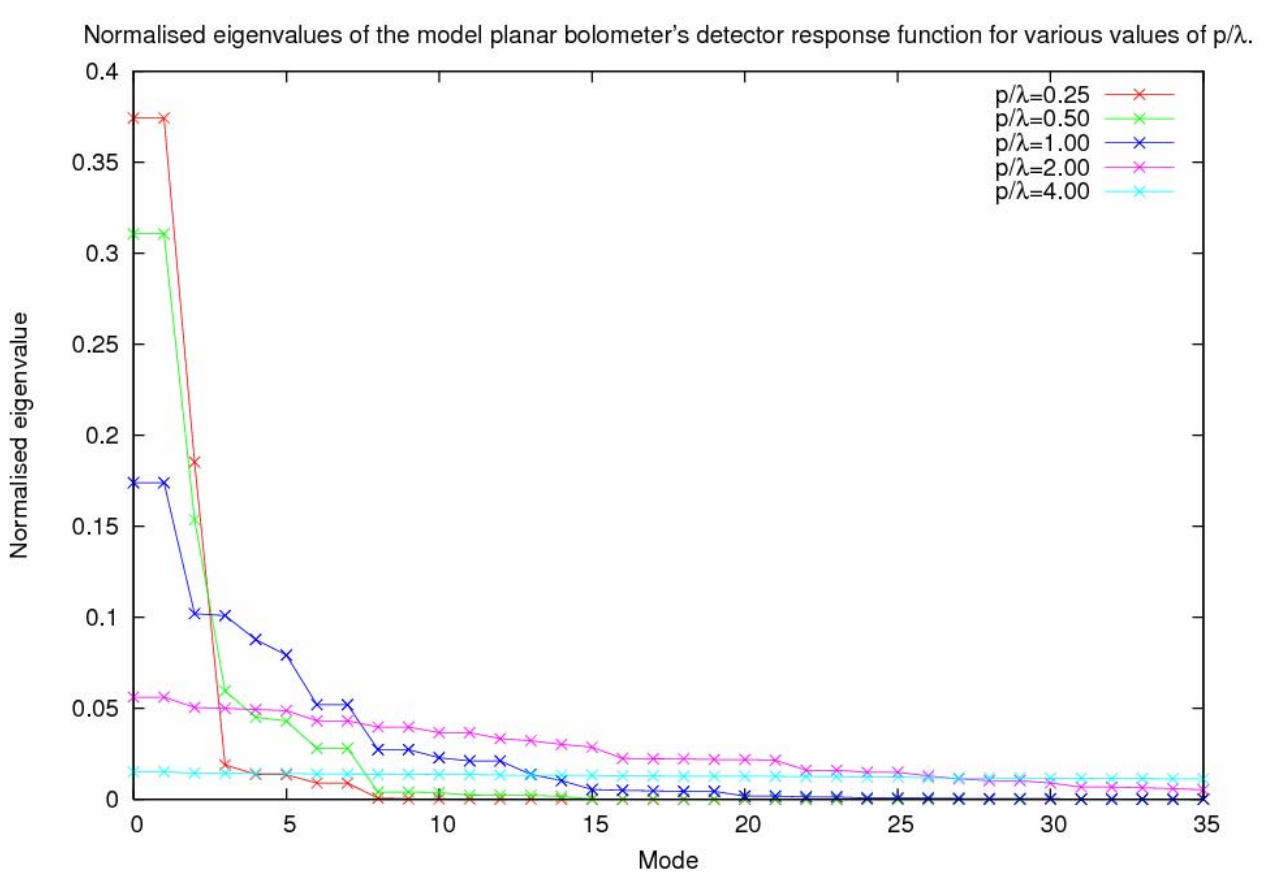

Fig. 7 Plot showing the normalised eigenvalues, $\{ \gamma^{(n)} / \Sigma_m \gamma^{(m)} \}$, of the detector response function of the model bolometer for different values of p/λ.. For each value of p/λ, the thirty-five largest normalised eigenvalues are shown.

belonging to a particularly set together with a line. This is to emphasise trends and to make it easier to distinguish between different sets. Remember that the normalised eigenvalues are a measure of the relative responsivity of the detector to the power in each of the modes. The higher the responsivity, the more the output of the detector depends on the power in the associated mode then the other modes. With this in mind we see that for values of $p/\lambda > 1$ the detector is equally responsive, approximately, to the power in all thirty-five modes shown. Intuitively this is what we would expect from an ideal absorber. It should be sensitive to the total power in the field independent of its exact spatial form. However for $p/\lambda < 1$ we observe very different behaviour. As p/λ decreases, the relative responsivity to the first three modes can be seen to increase while the responsivity to the other modes decreases. By $p/\lambda = 0.25$, the ideal bolometer essentially responds only to the power in three modes and is behaving as a few-mode detector.

This behaviour can be explained in terms of the apparent coherence length of the field over its surface that the absorber is sensitive to, which was discussed at the end of the previous section. From (18) we would expect this field to have zero coherence length. However, we noted that because of propagation effects the reception field that incident radiation 'sees' is actually coherent over spatial scales of at least ~λ, independent of the absorption mechanism. In the limit where the absorbing square is smaller then λ the reception field over the absorbing surface will therefore be coherent. As mentioned in section II, when the reception field is fully coherent the bolometer behaves like an antenna and will be single-moded. The reason we see actually see responsivity to three modes in this limit is in the proceeding discussion we have ignored the polarisation of the field. The three components of the field remain uncorrelated, so there are three such spatially fully-coherent modes possible. In the limit where $p/\lambda >> 1$, the field appears spatially incoherent on the scale of the absorber and we recover the ideal behaviour we had assumed.

Fig. 8 is a plot of the three far-field modes to which the detector is sensitive in the limit $p/\lambda << 1$. The details of the projection used are also shown in the figure. Notice that they correspond to the reception patterns expected for differently orientated electric dipole antennas, allowing for the additional zenith angle dependence already noted. The first two modes correspond to dipoles lying in the plane and are simply orthogonal polarisation states. The symmetry of the model bolometer in the x and y directions leads us to expect the bolometer should be equally responsive to both modes

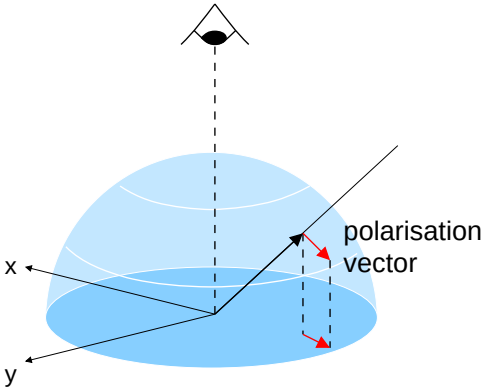

a) Details of projection used.

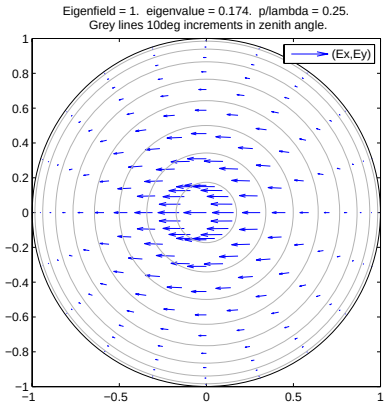

b) First mode (eigenvalue = 0.175)

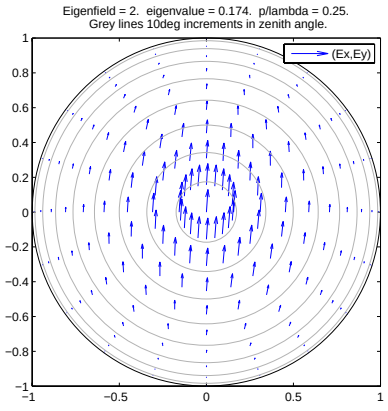

c) Second mode (eigenvalue = 0.175)

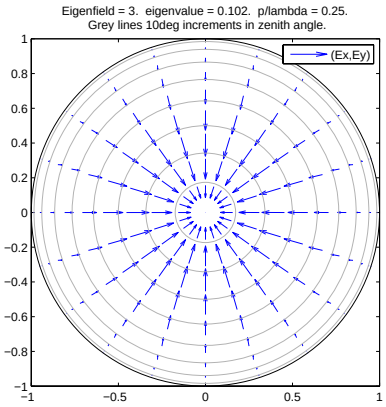

d) Third mode (eigenvalue = 0.102)

Fig. 8 The three modes of the incident field in which the bolometer is responsive to power at $p / \lambda = 0.25$. Panel (a) shows the detail of the projection used when plotting the fields. The polarisation vector associated with a particular direction of illumination is plotted at the point corresponding to the projection of the direction vector into the *(x, y)* plane. The polarisation vector is also shown projected into the plane, i.e. the vectors in the plot correspond to the *x* and *y* components of the polarisation vector in the coordinate system of Fig. 4. Panels (c) to (d) show the field plots. The grey circles indicate 10º increments in zenith angle.

and this is observed. It is slightly less responsive to the third mode, which corresponds to a dipole orientated normally to the bolometer plane. This is because the wave that would couple most effectively to it, a wave incident horizontally over the plane, is suppressed by the cosine dependence on zenith angle. These plots suggest a simple model for a diffraction limited planar absorber, consisting of three antennas with reduced responsivity to the dipole normal to the absorber.

CONCLUSIONS:

We have described a powerful technique for characterising and measuring the optical behaviour of bolometric detectors. A bolometer's behaviour is characterised by a quantity called the *detector response function*. This function essentially describes the set of fully-coherent modes in which the detector is simultaneously sensitive to power. We have shown that the response function can be determined experimentally by illuminating the detector with two coherent, phase-locked plane-wave sources operating at the same frequency. If the relative phase of the two waves is rotated, the visibility of the fringes at the output of the detector can be used to calculate the component of the response function for the particular polarisation and directions of incidence. By repeating for all pairs of source locations, and polarisation states, the full response function can be found.

This characterization process can be applied at any wavelength from the sub-millimetre, through the far-infrared and into the optical. The limiting factor is the ability to produce coherent, phase-locked, radiation at a particular wavelength. Furthermore, it can be applied independently of

the details of the power absorption mechanism, and how power is coupled into the detector. We envisage the procedure having uses outside of bolometer characterisation. The modes to which the detector is sensitive will depend on, for example, correlations and anisotropies in the absorber, relaxation processes and solid-state excitations. They should therefore be a source of information about these processes, and could be useful in solid-state physics and surface-physics.

We are intending to use these techniques to investigate planar absorbing structures at 195-270GHz, and have described an experiment that is currently being constructed. The theoretical models we have created suggest that planar absorbers should exhibit a change in behaviour from multi-mode to few-mode as the dimensions of the absorber fall below the wavelength of the radiation, or in situations where the absorption mechanism has some intrinsic sold-state coherence length, where the dimensions fall below this length. We expect to observe this behaviour experimentally.

Finally, in this paper we have only considered the response of detectors to fields in different states of spatial coherence. The illuminating radiation has been assumed to be stationary. In further work we hope to show that it is possible to recover the full spatio-temporal state of coherence of the incident field to which a detector is sensitive by performing the characterization with a pair of sources whose relative frequencies can be varied.

REFERENCES:

[1] M. J. Griffin, "Bolometers for far-infrared and submillimetre astronomy*", Nuclear Inst. and Methods in Physics Research A*, vol. 444, pp. 397–403, April 2000.

[2] G. Efstathiou, C. Lawrence and J. Tauber, "The Planck Blue Book", Planck Science Team, 2005.

[3] M. D. Audley and the CLOVER collaboration, "TES imaging array technology for CLOVER", in *Proc. SPIE*, vol. 6275, June 2006

[4] G. Saklatvala, S. Withington and M. P. S. Hobson, "Coupled-mode theory for infrared and submillimetre wave detectors*", J. Opt. Soc. Amer. A*, vol. 24, pp. 764–775, February 2007.

[5] S. Withington and G. Saklatvala, "Characterising the behaviour of partially coherent detectors through spatio-temporal modes", *J. Opt. A: Pure Appl. Opt.*, vol. 9, pp 626-633, April 2007.

[6] H. Griffiths and B. L. Smith, Ed., *Modern Antennas*, ser. Microwave and RF technology. London: Chapman & Hall, 1998.

[7] L. Mandel and E. Wolf, *Optical Coherence and Quantum Optics*, Cambridge University Press, 1995.

[8] M. Brand, "Fast online SVD revisions for lightweight recommender systems", in *Proceedings of the 3rd SIAM International Conference on Data Mining*, 2003.

[9] S. Withington, C. Y. Tham and G. Yassin, "Theoretical analysis of planar bolometric arrays for THz imaging systems", in *Proc. SPIE,* vol. 4855, pp. 49-62, 2003 .

[10] D. T. Chuss, E. J. Wollack, S. H. Moseley, S. Withington, and G. Saklatvala, "Diffraction considerations for planar detectors in the few-mode limit", *Publications of the Astronomical Society of the Pacific*, vol. 120, pp. 430-438, April 2008